

Host-derived, pore-forming toxin-like protein and trefoil factor complex protects the host against microbial infection

Yang Xiang^{a,1}, Chao Yan^{a,b,1}, Xiaolong Guo^{a,b}, Kaifeng Zhou^{a,b}, Sheng'an Li^a, Qian Gao^a, Xuan Wang^{a,b}, Feng Zhao^{a,b}, Jie Liu^{a,b}, Wen-Hui Lee^a, and Yun Zhang^{a,2}

^aKey Laboratory of Animal Models and Human Disease Mechanisms, The Chinese Academy of Sciences and Yunnan Province, Kunming Institute of Zoology, Chinese Academy of Sciences, Kunming, Yunnan 650223, China; and ^bKunming College of Life Science, University of Chinese Academy of Sciences, Beijing 100049, China

Edited by B. Brett Finlay, University of British Columbia, Vancouver, BC, Canada, and accepted by the Editorial Board March 26, 2014 (received for review November 18, 2013)

Aerolysins are virulence factors belonging to the bacterial β -pore-forming toxin superfamily. Surprisingly, numerous aerolysin-like proteins exist in vertebrates, but their biological functions are unknown. $\beta\gamma$ -CAT, a complex of an aerolysin-like protein subunit (two $\beta\gamma$ -crystallin domains followed by an aerolysin pore-forming domain) and two trefoil factor subunits, has been identified in frogs (*Bombina maxima*) skin secretions. Here, we report the rich expression of this protein, in the frog blood and immune-related tissues, and the induction of its presence in peritoneal lavage by bacterial challenge. This phenomena raises the possibility of its involvement in antimicrobial infection. When $\beta\gamma$ -CAT was administered in a peritoneal infection model, it greatly accelerated bacterial clearance and increased the survival rate of both frogs and mice. Meanwhile, accelerated Interleukin-1 β release and enhanced local leukocyte recruitments were determined, which may partially explain the robust and effective antimicrobial responses observed. The release of interleukin-1 β was potentially triggered by $\beta\gamma$ -CAT from the frog peritoneal cells and murine macrophages *in vitro*. $\beta\gamma$ -CAT was rapidly endocytosed and translocated to lysosomes, where it formed high molecular mass SDS-stable oligomers (>170 kDa). Lysosomal destabilization and cathepsin B release were detected, which may explain the activation of caspase-1 inflammasome and subsequent interleukin-1 β maturation and release. To our knowledge, these results provide the first functional evidence of the ability of a host-derived aerolysin-like protein to counter microbial infection by eliciting rapid and effective host innate immune responses. The findings will also largely help to elucidate the possible involvement and action mechanisms of aerolysin-like proteins and/or trefoil factors widely existing in vertebrates in the host defense against pathogens.

innate immunity | infectious disease | interleukin-1beta

The eradication of invading microorganisms is essential for the survival of vertebrates, including frogs. Innate antimicrobial responses play a key role in host defense against many infections (1). Host innate immune cells, such as neutrophils, monocytes, and macrophages, can be activated by various cytokines to engulf pathogens and release toxic oxygen and nitrogen radicals (2). Interleukin-1 β (IL-1 β) is one of the key cytokines that initiate and amplify a wide variety of effects associated with the host response to microbial invasion (3, 4). The strategies and molecular identities of such host endogenous regulators that ensure rapid, effective, and controllable antimicrobial responses are incompletely understood (2, 5–7).

The frog species *Bombina maxima* lives in very harsh environments, such as pools containing microorganism-rich mud, and its skin is very “toxic.” Our previous study demonstrated that *B. maxima* possesses an immune system similar to that of mammals (8). A 72-kDa complex of bacterial pore-forming toxin (PFT) aerolysin-like protein (α -subunit) and trefoil factor (TFF) (β -subunit)

with a noncovalently linked form of $\alpha\beta_2$ was recently identified in the skin secretions of this species. The α -subunit is composed of an aerolysin domain fused to two N-terminal $\beta\gamma$ -crystallin domains (9–11). The β -subunit is a three-domain TFF (Fig. 1A). This protein complex was therefore named $\beta\gamma$ -CAT to reflect its domain composition.

For the purpose of invasion, several pathogenic bacteria produce PFTs, such as β -barrel-type aerolysins, which can oligomerize and form pores in host-cell membranes (12, 13). The aerolysin domain is defined according to its structural similarity to the transmembrane domain of aerolysin toxins. Strikingly, a diverse array of proteins harboring an aerolysin domain fused with other domains have been identified in various vertebrate species (9). Similar to the α -subunit of $\beta\gamma$ -CAT, ep37 proteins from the amphibian newt *Cynops pyrrhogaster* harbor an aerolysin domain fused to two N-terminal $\beta\gamma$ -crystallin domains that share structural similarity with eye lens $\beta\gamma$ -crystallins (14). TFFs are characterized by one to four trefoil domains, which are highly conserved among TFF proteins, from frogs to humans. These proteins are constitutively released within the mucosal layer that covers the gastrointestinal, urinary, respiratory, and skin surfaces and are believed to play pivotal roles in mucosal barrier function

Significance

Pore-forming toxins are a common type of bacterial toxins and are important bacterial virulence factors. Aerolysin is produced by *Aeromonas* species. It is interesting that aerolysin-like proteins are also found in vertebrates. However, the physiological roles of these proteins are still unknown. Previously, a $\beta\gamma$ -crystallin fused aerolysin-like protein (α -subunit) and trefoil factor (β -subunit) complex, hence named $\beta\gamma$ -CAT, was identified in frogs. Here, we found that this complex is inducible by bacterial challenge. The complex was able to protect the host from microbial infection. It oligomerized along the endosome pathway to trigger lysosome destabilization and led to interleukin-1 β maturation and secretion via inflammasome activation. Our present work provides functional evidence for uncovering the physiological roles of vertebrate-derived bacterial pore-forming toxin-like proteins.

Author contributions: Y.X. and Y.Z. designed research; Y.X., C.Y., X.G., K.Z., S.L., and J.L. performed research; Q.G. and X.W. contributed new reagents/analytic tools; Y.X., C.Y., X.G., S.L., Q.G., F.Z., W.-H.L., and Y.Z. analyzed data; and Y.X. and Y.Z. wrote the paper.

The authors declare no conflict of interest.

This article is a PNAS Direct Submission. B.B.F. is a guest editor invited by the Editorial Board.

¹Y.X. and C.Y. contributed equally to this work.

²To whom correspondence should be addressed. E-mail: zhangy@mail.kiz.ac.cn.

This article contains supporting information online at www.pnas.org/lookup/suppl/doi:10.1073/pnas.1321317111/-DCSupplemental.

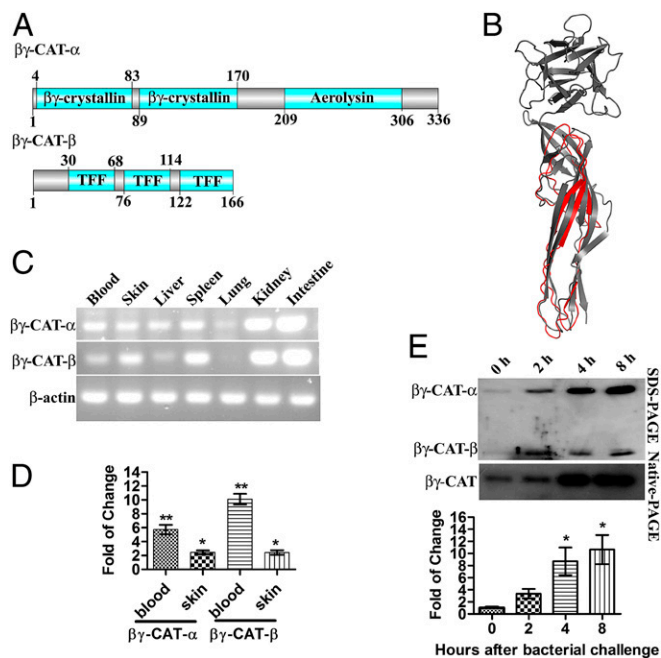


Fig. 1. $\beta\gamma$ -CAT possesses an aerolysin domain and can be induced by bacterial challenge. (A) Schematic structure of $\beta\gamma$ -CAT. A $\beta\gamma$ -CAT molecule contains one α -subunit and two β -subunits. One α -subunit contains two $\beta\gamma$ -crystallin domains and one aerolysin domain, and one β -subunit contains three trefoil domains. (B) The model of the $\beta\gamma$ -CAT aerolysin domain in 3D based on the crystal structure of the hemolytic lectin from the mushroom *L. sulphureus* (PDB ID code 1w3g), which harbors an aerolysin domain at the C terminus. The structure was predicted by the I-TASSER server. The predicted aerolysin domain of $\beta\gamma$ -CAT is shown in red, and the hemolytic lectin from the mushroom *L. sulphureus* is shown in gray. The picture was generated by the PyMOL program (for Windows). (C) Expression profile of $\beta\gamma$ -CAT in different organs. (D) The $\beta\gamma$ -CAT mRNA level was up-regulated 24 h after being fed in a bacteria-containing environment (*Comamonas* sp., 1×10^8 cfu/mL). (E) Frogs were intraperitoneally injected with bacteria (*Comamonas* sp., 1×10^8 cfu per frog in 100 μ L), and the peritoneal fluids were harvested by 2 mL of 0.9% NaCl and concentrated to 100 μ L by lyophilization. The protein level of $\beta\gamma$ -CAT in the frog peritoneum was assessed by Western blotting after SDS/PAGE (Top, 10 μ L per lane) and native-PAGE (Middle, 10 μ L per lane). The amount of $\beta\gamma$ -CAT (after native-PAGE) was also semiquantified (Fig. S1B), and the fold of change was presented (Bottom). The data in D and E represent the mean \pm SD of triplicate samples. * $P < 0.05$ and ** $P < 0.01$ by Student *t* test. The other data are representative of at least two independent experiments.

and repair (15–17). In particular, TFF2 has been shown to be essential in the regulation of IL-33 release at mucosal surfaces (18). Increased susceptibility to *Yersinia enterocolitica* was found in TFF2-knockout mice, which died following infection (19).

Previously, it was observed that $\beta\gamma$ -CAT causes species-specific hemolysis that is blocked by osmoprotectants, demonstrating its membrane pore formation properties (10, 11). However, the complex's biological functions and its associated mechanisms remain elusive. In vivo injection of $\beta\gamma$ -CAT induces strong proinflammatory responses (20), and the protein has been detected in the skin and gastrointestinal tract of *B. maxima* (10). These findings led to the hypothesis that the protein might be involved in host defense against microbial invasion. In the present study, $\beta\gamma$ -CAT was found to significantly accelerate bacterial clearance, thus reducing the mortality rate in *B. maxima* frog and mouse peritonitis models. The rapid maturation and release of IL-1 β triggered by $\beta\gamma$ -CAT were detected both in vivo and in vitro and may have resulted from the oligomerization of, and pore formation by, the protein within cellular lysosomes.

Results

Frog $\beta\gamma$ -CAT α -Subunit Is a Bacterial Pore-Forming Toxin-Like Protein.

The domain architecture of $\beta\gamma$ -CAT has been previously described (10). Its α -subunit contains an aerolysin domain at the C terminus (Fig. 1A). Modeling of the aerolysin domain of $\beta\gamma$ -CAT in 3D showed that it is similar to the aerolysin domain of the hemolytic lectin from the mushroom *Laetiporus sulphureus*, with a confidence score (C-score) of -0.74 (Fig. 1B). Indeed, the aerolysin domain-containing proteins are widely distributed, from bacteria to vertebrates (9) (Table S1). Specifically, the aerolysin domain of $\beta\gamma$ -CAT showed high similarity to the aerolysin domains of other vertebrate proteins (Fig. S1A). However, few other vertebrate-derived aerolysin-like proteins have been purified and characterized. A sufficient amount of the $\beta\gamma$ -CAT protein could be purified and characterized from *B. maxima* skin secretions, allowing us to explore its physiological and pathological functions without genetic manipulation, which is very hard to perform in *B. maxima*.

$\beta\gamma$ -CAT Is Inducible During Bacterial Infection. RT-PCR of the $\beta\gamma$ -CAT α -subunit and β -subunit revealed that each subunit was constitutively expressed in the skin, spleen, kidney, and intestine of frogs (Fig. 1C). These organs possess immune functions in amphibians. Skin and blood from frogs fed in bacterium-rich water showed up-regulated mRNA levels of both subunits of $\beta\gamma$ -CAT (Fig. 1D). A peritonitis model was also used to test whether $\beta\gamma$ -CAT was induced during i.p. infection. The presence of bacteria (*Comamonas* sp.) significantly up-regulated $\beta\gamma$ -CAT at 2, 4, and 8 h postchallenge (Fig. 1E). The amount of $\beta\gamma$ -CAT produced in the peritoneum after bacterial challenge is semiquantified (Fig. S1B). The $\beta\gamma$ -CAT produced at 4 and 8 h after bacterial challenge was estimated to be 0.33 ± 0.16 μ g and 0.40 ± 0.21 μ g, which could result in the concentrations of $\beta\gamma$ -CAT in 100- μ L peritoneum fluids to be 46 ± 22 nM and 56 ± 29 nM, respectively.

$\beta\gamma$ -CAT Protects Frogs and Mice Against Bacterial Infection. Because $\beta\gamma$ -CAT was inducible during bacterial challenge, it was hypothesized that this complex plays an important role in antimicrobial immune responses. A frog peritonitis model was used to test this hypothesis. A conditional pathogenic bacterium, *Comamonas* sp., isolated from the skin of *B. maxima* (Table S2), was used to test the influence of $\beta\gamma$ -CAT on bacterial infection. Intraperitoneal injection of the bacterium resulted in infection and death of frogs. However, $\beta\gamma$ -CAT injection 4 h before the bacterial injection significantly reduced frog mortality (Fig. 2A). $\beta\gamma$ -CAT reduced the bacterial load in the frog peritoneum at 24, 48, and 72 h after infection (Fig. 2B). $\beta\gamma$ -CAT had no direct killing and/or inhibiting effects on bacteria, including *Comamonas* sp. (Table S3). The absence of direct antimicrobial function of $\beta\gamma$ -CAT suggests that it might stimulate antimicrobial immune responses in vivo. Subsequently, peritoneal exudates cells were analyzed by flow cytometry. Unfortunately, no specific antibodies that can distinguish different types of cells in *B. maxima* are currently available, and we could therefore discern cell populations only by forward scatter (FSC) and side scatter (SSC) (Fig. 2C). The results showed that the percentage of the cells in a subpopulation was elevated at 2 and 4 h after $\beta\gamma$ -CAT injection. This subpopulation of the cells was stained with Wright's stain, and the cells showed monocytic morphology (Fig. 2D). Additionally, IL-1 β levels after $\beta\gamma$ -CAT injection were examined in the peritoneum by Western blotting. The results showed that $\beta\gamma$ -CAT promoted the maturation and secretion of IL-1 β at 0.5, 1, 2, and 4 h after the i.p. injection of $\beta\gamma$ -CAT (Fig. 2E).

The in vivo effects of $\beta\gamma$ -CAT in mice were similar to those in frogs, including an improvement of the survival rate (Fig. 2F for *Escherichia coli* strain ATCC 25922 and Fig. S2A for *Staphylococcus aureus* strain ATCC 25923) and an enhancement of bacterial clearance (Fig. S2B and C). Cytokine production in the

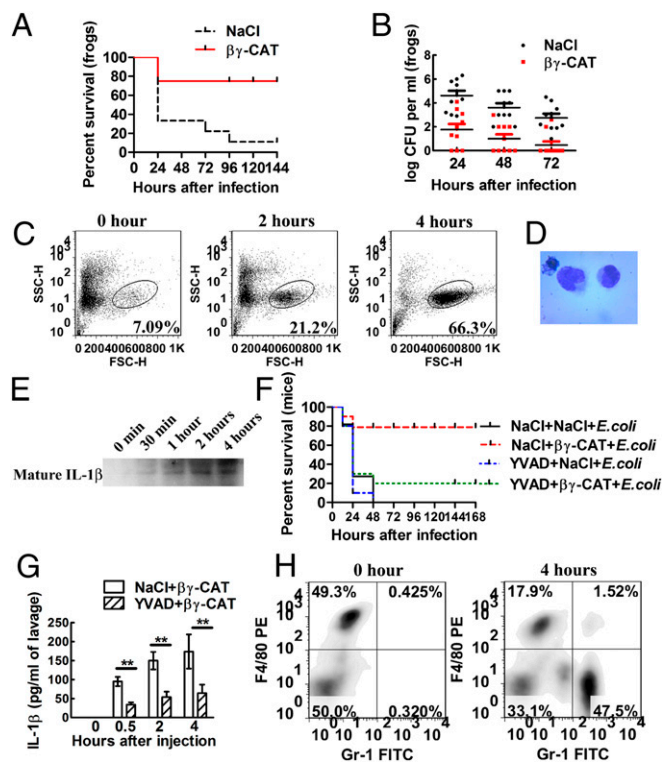


Fig. 2. $\beta\gamma$ -CAT protects animals against bacterial infection. (A) Frogs (*B. maxima*) weighing 25 ± 5 g were injected intraperitoneally with 1×10^9 cfu of bacteria (*Comamonas* sp.) to induce peritonitis. *B. maxima* mortality was then observed every 24 h. Moreover, to assess the influence of $\beta\gamma$ -CAT on bacterial infection, 40 $\mu\text{g}/\text{kg}$ $\beta\gamma$ -CAT was intraperitoneally injected 4 h before infection. (B) Frogs (*B. maxima*) weighing 25 ± 5 g were injected intraperitoneally with 1×10^8 cfu of bacteria (*Comamonas* sp.). The number of peritoneal bacteria was then counted every 24 h after infection. Furthermore, to assess the influence of $\beta\gamma$ -CAT on bacterial infection, 40 $\mu\text{g}/\text{kg}$ $\beta\gamma$ -CAT was intraperitoneally injected 4 h before infection. (C) Frogs were intraperitoneally injected with 40 $\mu\text{g}/\text{kg}$ $\beta\gamma$ -CAT, and the peritoneal exudates cells were harvested for flow cytometry analysis. The increased subpopulation of the cells is indicated. (D) The increased subpopulation of the cells was stained and photographed and showed monocytic morphology. (E) Frogs were intraperitoneally injected with 40 $\mu\text{g}/\text{kg}$ $\beta\gamma$ -CAT, and the peritoneal fluids were harvested by 2 mL of 0.9% NaCl and concentrated to 100 μL by lyophilization. The fluids were then immunoblotted using rabbit polyclonal antibodies against *B. maxima* IL-1 β . (F) Four-week-old male Kunming mice were intraperitoneally infected with *E. coli* (ATCC 25922), and the mortality was assessed every 12 h. Mice were also intraperitoneally injected with 25 $\mu\text{g}/\text{kg}$ $\beta\gamma$ -CAT to assess the complex's role in the mortality. Additionally, a caspase-1 inhibitor, Ac-YVAD-cmk (5 mg/kg), was injected 1 h before $\beta\gamma$ -CAT injection to assess the role of caspase-1 and the inflammasome in mouse mortality. (G) Mice were injected intraperitoneally with $\beta\gamma$ -CAT (25 $\mu\text{g}/\text{kg}$), and the concentration of IL-1 β was assessed at the indicated time points in mouse peritoneal fluids by ELISA. Moreover, the caspase-1 inhibitor Ac-YVAD-cmk (5 mg/kg) was injected 1 h before $\beta\gamma$ -CAT injection to assess the role of caspase-1 in IL-1 β secretion. (H) The proportion of neutrophils was assessed by double staining with anti-Gr-1-FITC and anti-F4/80-PE antibodies. Gr-1^{high} F4/80^{low} neutrophils were attracted to the peritoneum 4 h after $\beta\gamma$ -CAT injection. The survival rate and bacterial count data are representative of two experiments, with $n = 10$ frogs or mice per group. The flow-cytometry data are representative of at least two experiments, with six frogs or three mice each. The ELISA data represent the mean \pm SD of triplicate samples. $**P < 0.01$ by Student *t* test. The other data are representative of at least two independent experiments. See also Fig. S2.

mouse peritoneum after $\beta\gamma$ -CAT injection was assayed. The levels of IL-1 β (Fig. 2G) and chemokines such as CXCL1 (Fig. S2D) and CXCL2 (Fig. S2E) were elevated. Moreover, 4 h after $\beta\gamma$ -CAT injection, the percentage of neutrophils (Gr-1^{high} F4/80^{low})

was markedly elevated (Fig. 2H). The difference in leukocyte recruitment between frogs and mice may result from differences in their leukocyte profiles. Due to the lack of a specific inhibitor for frog caspase-1, it is difficult to accurately evaluate the role of caspase-1 in the biological effect of $\beta\gamma$ -CAT. However, all of these effects in mice could be attenuated by the preadministration of Ac-YVAD-cmk, a caspase-1 inhibitor (Fig. 2F and G and Fig. S2B–E). Therefore, it was inferred that caspase-1 may also be a downstream regulator of $\beta\gamma$ -CAT in *B. maxima*.

All of these results revealed the positive role of $\beta\gamma$ -CAT in triggering antimicrobial responses against bacterial infection.

$\beta\gamma$ -CAT Induces Inflammasome-Dependent IL-1 β Secretion. The above *in vivo* experiments in frogs and mice showed that $\beta\gamma$ -CAT induced IL-1 β secretion. Moreover, a previous study demonstrated that aerolysin can activate the inflammasome and caspase-1 (21). Thus, it is reasonable to hypothesize that $\beta\gamma$ -CAT plays a role in activating the inflammasome and that the antimicrobial effect of $\beta\gamma$ -CAT is at least partially dependent on inflammasome and caspase-1 activation.

Up to 400 nM $\beta\gamma$ -CAT showed no cytotoxicity to frog peritoneal cells (Fig. 3A). LPS-primed frog peritoneal cells secreted IL-1 β at 0.5, 1, and 2 h after stimulation with 100 nM $\beta\gamma$ -CAT (Fig. 3C, Upper). However, $\beta\gamma$ -CAT did not induce IL-1 β expression, as shown by its stable mRNA levels detected by RT-PCR (Fig. 3B). Thus, the role of $\beta\gamma$ -CAT in promoting IL-1 β secretion may primarily be to accelerate the maturation process. Additionally, Western blotting for caspase-1 revealed that the matured p20 subunit was present in the lysate of *B. maxima* peritoneal cells at 0.5, 1, and 2 h after $\beta\gamma$ -CAT stimulation (Fig. 3C, Lower).

NLRP1, NLRP3, and AIM2 inflammasomes are upstream protein complexes that activate caspase-1. We assessed the biological effect of $\beta\gamma$ -CAT on mouse bone marrow-derived macrophages (BMDMs), and similar results were obtained. $\beta\gamma$ -CAT (5 nM) stimulated IL-1 β secretion (Fig. 3E). Mature IL-1 β was detected by Western blotting (Fig. 3D, Upper), and caspase-1 was activated 0.5 h after $\beta\gamma$ -CAT stimulation (Fig. 3D, Lower). Knockdown of caspase-1, ASC, and NLRP3 attenuated $\beta\gamma$ -CAT-induced IL-1 β secretion (Fig. 3F and Fig. S3B). However, knockdown of NLRP3 had no influence on IL-1 β secretion. This result indicated that $\beta\gamma$ -CAT activates caspase-1 through activation of the NLRP3 inflammasome. Whether $\beta\gamma$ -CAT has the same effect on *B. maxima* requires further detailed study.

$\beta\gamma$ -CAT Endocytosis and Lysosome Destabilization Play Pivotal Roles in Its Function. The above results mentioned in *$\beta\gamma$ -CAT Induces Inflammasome-Dependent IL-1 β Secretion* suggest that $\beta\gamma$ -CAT triggers caspase-1 activation by inducing the assembly of the inflammasome, but the mechanism by which the protein activates the inflammasome is unknown. Previous studies demonstrated that exposure of endothelial cells to $\beta\gamma$ -CAT results in its rapid endocytosis and oligomerization and that endocytosis is required for the complex's biological activity (10). Thus, in the present study, we sought to determine whether endocytosis is important in IL-1 β release.

B. maxima peritoneal cells incubated with 100 nM $\beta\gamma$ -CAT exhibited oligomerization of $\beta\gamma$ -CAT (Fig. 4A), similar to the results previously observed in endothelial cells. The subcellular localization of $\beta\gamma$ -CAT was assessed, and the results revealed that $\beta\gamma$ -CAT was enriched in the endolysosomal fraction (Fig. 4B). Both the oligomerized $\beta\gamma$ -CAT and the $\beta\gamma$ -CAT α -subunit could be detected by an anti- $\beta\gamma$ -CAT antibody; however, its β -subunit appeared to be missing in this fraction. The β -subunit may serve as an adaptor protein for receptor recognition and may be degraded after ligand-receptor binding and $\beta\gamma$ -CAT endocytosis. A colocalization experiment was also carried out in mouse BMDMs, and the results showed that most of the endocytosed $\beta\gamma$ -CAT colocalized with the lysosomal marker Lamp-1

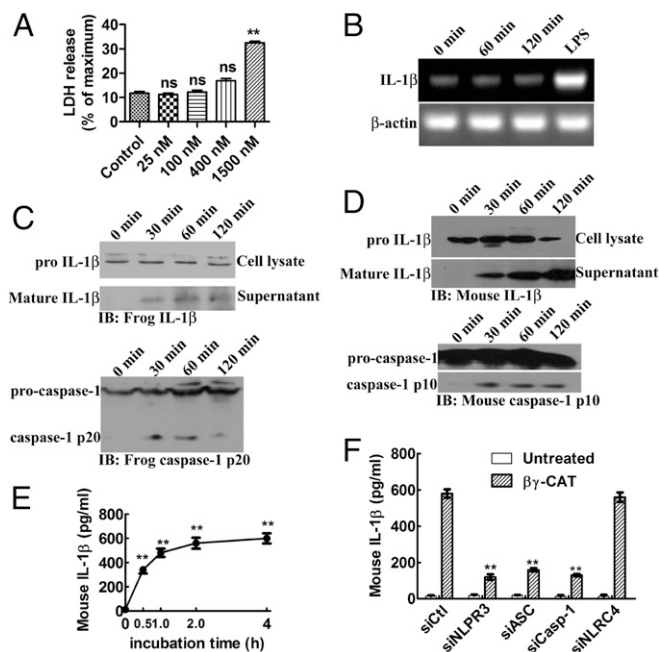


Fig. 3. $\beta\gamma$ -CAT induces IL-1 β secretion, which may result from caspase-1 inflammasome activation. (A) Frog peritoneal cells were treated with different concentrations of $\beta\gamma$ -CAT for 2 h, and cytotoxicity was determined using an LDH release assay. (B) Frog peritoneal cells were treated with $\beta\gamma$ -CAT (100 nM) for 1–2 h or LPS (100 ng/mL) for 2 h. The expression of IL-1 β was then detected by RT-PCR. See also Fig. S3A for the result of mouse BMDMs. (C) Frog peritoneal cells were primed with LPS (100 ng/mL) and incubated with $\beta\gamma$ -CAT (100 nM) for 30 min to 2 h. The cells were then lysed to detect pro-IL-1 β , and culture supernatants were concentrated to detect mature IL-1 β by immunoblotting with a rabbit polyclonal antibody against *B. maxima* IL-1 β . Caspase-1 and activated subunit p20 in the cell lysate were also detected by immunoblotting using a rabbit polyclonal antibody against *B. maxima* caspase-1 p20. (D) Lysates and supernatants from LPS-primed mouse BMDMs stimulated with $\beta\gamma$ -CAT (5 nM) for the indicated times were immunoblotted with an antibody against the p10 subunit of caspase-1 and with an antibody against IL-1 β . (E) The IL-1 β concentration in the supernatant obtained in D was measured by ELISA. (F) Mouse BMDM NLRP3, ASC, caspase-1, or NLRP4 was knocked down by siRNA, and the cells were then treated with $\beta\gamma$ -CAT (5 nM) for 2 h. Culture supernatants were then collected, and released IL-1 β was measured by ELISA. The knockdown of these proteins was confirmed by Western blotting (Fig. S3B). The LDH releasing and ELISA data represent the mean \pm SD of triplicate samples. ns, No significance. $^{***}P < 0.01$ by Student *t* test. The other data are representative of at least two independent experiments.

(Fig. 4C). Cytochalasin D and nocodazole reduced the presence of $\beta\gamma$ -CAT in the endolysosomal fraction (Fig. 4D), indicating that microtubules and actin filaments are essential for efficient transporting of $\beta\gamma$ -CAT to lysosomes. Consequently, $\beta\gamma$ -CAT-induced IL-1 β secretion was largely inhibited in the presence of cytochalasin D or nocodazole (Fig. 4E). ATP is a well-known inducer of IL-1 β secretion by acting on a plasma membrane receptor (p2x7) without entering the cells (22). In the control assay, cytochalasin D did not affect ATP-triggered IL-1 β secretion whereas nocodazole partially inhibited ATP-induced IL-1 β secretion due to the role of microtubules on NLRP3 inflammasome-dependent IL-1 β secretion (23) (Fig. 4E). In addition, bafilomycin A1, a vacuolar-type ATPase inhibitor that could block the pathway from the early to late endosome, strongly inhibited $\beta\gamma$ -CAT-induced IL-1 β secretion but showed no obvious effect on that triggered by ATP. Taken together, these results indicate that endocytosis and being targeted to endolysosomes are necessary for the function of $\beta\gamma$ -CAT. Oligomerization and pore formation of $\beta\gamma$ -CAT in endolysosomes may

destabilize the lysosome. The frog cells were stained with acridine orange to examine the status of the lysosome. The results showed that $\beta\gamma$ -CAT induced lysosomal instability because it reduced the acidity of the intracellular acidic compartment (Fig. 4F). Lysosomal destabilization is sufficient to activate the inflammasome (24). This effect is achieved by the release of cathepsin B from the lysosome into the cytosol. In this line, it was found that $\beta\gamma$ -CAT stimulation resulted in the translocation of cathepsin B into the cytosolic fraction (Fig. 4G). A cathepsin B inhibitor, CA074-Me, was able to reduce $\beta\gamma$ -CAT-induced IL-1 β secretion in *B. maxima* peritoneal cells (Fig. 4E). Similar results were also obtained in mouse BMDMs (Fig. S4).

Discussion

Frog skin is naked and constantly confronted by a complex mixture of potentially infectious microbes. Microbial invasion and infection due to disruptions of the surface cell layer occur frequently (25). To our knowledge, $\beta\gamma$ -CAT is the first example of a naturally existing complex of bacterial PFT-like protein and TFF in vertebrates (10, 11). In contrast to small molecular-weight antimicrobial peptides from the same frog species (26, 27), $\beta\gamma$ -CAT neither directly kills bacteria nor inhibits their growth (Table S3). The present study elucidated the complex's capacity to stimulate potent antimicrobial responses both in frog *B. maxima* and in mice, resulting in effective protection against lethal bacterial infection. $\beta\gamma$ -CAT was found in the skin, on the luminal surfaces of the intestine and stomach, and in immune-related organs, suggesting a role for $\beta\gamma$ -CAT in immunity. In addition, the protein's levels were significantly increased in peritoneal fluids after bacterial challenge. The amounts of $\beta\gamma$ -CAT produced endogenously, as estimated in Fig. S1B, should be sufficient to activate the frog cells to release IL-1 β and to trigger antimicrobial responses (Fig. 3). Taken together, these results suggest a sentinel role of $\beta\gamma$ -CAT in preventing pathogen invasion. It is worthy of pointing out that this protein is expressed in frogs even in the absence of infection. This fact suggests that its effects must be tightly regulated. Several possibilities may exist in frogs. At first, the inhibitory proteins of $\beta\gamma$ -CAT may exist extracellularly and/or intracellularly when the host is not infected by pathogens. Upon infection, the down-regulation of these unknown specific inhibitory proteins of $\beta\gamma$ -CAT may facilitate $\beta\gamma$ -CAT to exert its functions. Second, because the action of $\beta\gamma$ -CAT is membrane receptor-mediated (10), the timely and spatially regulated expression of putative $\beta\gamma$ -CAT receptor(s) in different cell types may also modulate the action of $\beta\gamma$ -CAT. As an exogenous factor to mice, these regulatory mechanisms normally present in frogs might be inefficient or even absent in mice. This notion is consistent with the fact that a higher concentration (100 nM) of $\beta\gamma$ -CAT was used for activating IL-1 β secretion in the peritoneal cells of frogs than that (5 nM) used in mouse BMDMs (Fig. 3). The illustration of the mechanisms that regulate the action of $\beta\gamma$ -CAT is an interesting future challenge.

IL-1 β activation is controlled not only by transcription but also by a proteolytic pathway that is mainly under the control of inflammasomes (5, 28). Cell stimulation with Toll-like receptor (TLR) ligands, such as LPS, is required to induce the transcription of IL-1 β mRNA and the production of pro-IL-1 β protein. A second signal is required to trigger inflammasome activation and the subsequent rapid and efficient processing of mature IL-1 β and its release (28). $\beta\gamma$ -CAT clearly did not enhance the transcription of IL-1 β in either frogs or mice (Fig. 3B and Fig. S3A) although the protein rapidly triggered IL-1 β release. This phenomenon suggests that, in contrast to microbial TLR ligands, the protein primarily acts as a second signal to stimulate IL-1 β maturation and release, which have been shown to be NLRP3 inflammasome-dependent in mice. The immune system of frogs shows a high degree of similarity and evolutionary conservation with that of mammals (29). Transcriptome sequencing revealed

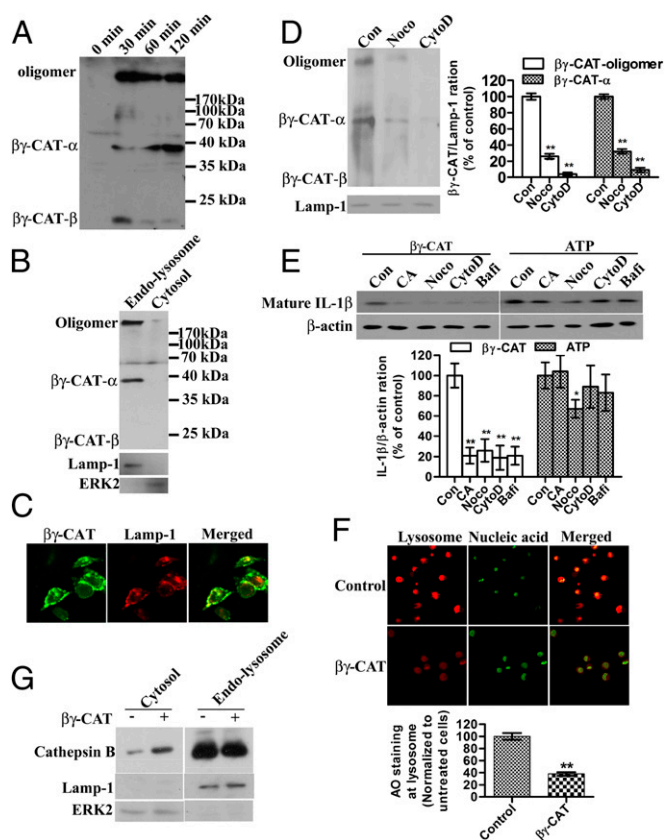


Fig. 4. $\beta\gamma$ -CAT endocytosis and lysosome destabilization induce IL-1 β secretion. (A) Frog peritoneal cells were treated with $\beta\gamma$ -CAT (100 nM) for 30 min to 2 h. The cells were then lysed for Western blotting detection of $\beta\gamma$ -CAT. (B) Frog peritoneal cells were treated with $\beta\gamma$ -CAT (100 nM) for 30 min and then lysed. The cytosolic fraction and endolysosomal fraction were prepared, and the distribution of $\beta\gamma$ -CAT was assessed by Western blotting. Lamp-1 was used as the marker of the endolysosomal fraction, and ERK2 was used as the marker of the cytosolic fraction. (C) Mouse BMDMs were treated with $\beta\gamma$ -CAT (5 nM) for 30 min and then stained with an anti- $\beta\gamma$ -CAT antibody (green) and an anti-Lamp-1 antibody (lysosome marker) (red). $\beta\gamma$ -CAT was colocalized with Lamp-1. (D) Frog peritoneal cells were pretreated with cytochalasin D (CytoD, 2 μ M) or nocodazole (Noco, 10 μ M) for 30 min before incubated with $\beta\gamma$ -CAT (100 nM) for 30 min and then lysed. The endolysosomal fraction was prepared. $\beta\gamma$ -CAT was assessed by Western blotting. $\beta\gamma$ -CAT transported to endolysosomal fraction was quantified with ImageJ. (E) Frog peritoneal cells were pretreated with CA074-Me (CA, 30 μ M), cytochalasin D (CytoD, 2 μ M), nocodazole (Noco, 10 μ M), or bafilomycin A1 (Bafi, 25 nM) for 30 min and then incubated with $\beta\gamma$ -CAT (100 nM) or ATP (5 mM) for 2 h. The IL-1 β concentration in the supernatants was assessed by Western blotting for *B. maxima* IL-1 β . Cells were lysed for Western blotting detection of β -actin, serving as a loading control. Bands were semiquantified with ImageJ. (F) $\beta\gamma$ -CAT-treated (100 nM for 30 min) or untreated frog peritoneal cells were stained with acridine orange (AO), and intact lysosomes were visualized using a Zeiss LSM510 microscope (red). The fluorescence intensity of the acidic compartment was quantified using ImageJ software. (G) $\beta\gamma$ -CAT-treated (100 nM for 30 min) or untreated frog peritoneal cells were lysed, and the cytosolic and endolysosomal fractions were prepared. The leakage of cathepsin B from the lysosome into the cytosol was then assessed by Western blotting for cathepsin B. The data in D, E, and F represent the mean \pm SD of triplicate samples. * $P < 0.05$ and ** $P < 0.01$ by Student *t* test. The other data are representative of at least two independent experiments. See also Fig. S4.

that most inflammasome-related elements are conserved in *B. maxima*, such as NLRP proteins, caspases, and IL-1 β (8), suggesting that $\beta\gamma$ -CAT also triggers IL-1 β maturation and release in frogs via inflammasomes.

Our results indicated that endocytosis and transportation of $\beta\gamma$ -CAT to lysosomes is required for $\beta\gamma$ -CAT-stimulated IL-1 β

maturation and secretion. NLR-dependent (NLRP3-dependent in mammals) caspase-1 activation and IL-1 β release have been associated with destabilization of the lysosomal membrane and activation of lysosomal proteases (specifically, cathepsin B) (6). The $\beta\gamma$ -CAT α -subunit consists of structural elements that tend to undergo oligomerization and insert into the membrane to form pores (9, 30, 31). Previous studies have shown that, whereas the β -subunit of $\beta\gamma$ -CAT is most likely responsible for binding to cells via “protein” receptor(s), its α -subunit formed transmembrane pores in anucleate erythrocyte and platelet membranes, which resulted in rapid K⁺ efflux (10, 11, 32). In the present study, endocytosis and the formation of high molecular mass oligomers (>170 kDa) of $\beta\gamma$ -CAT in lysosomes were observed in frog cells. These events could lead to destabilization of the lysosomal membrane by ion-flux disturbance, which may eventually result in inflammasome activation and subsequent IL-1 β maturation and release. Although the α -subunit of $\beta\gamma$ -CAT is a bacterial PFT-like protein, the mechanism by which $\beta\gamma$ -CAT activates the inflammasome is completely different from that of aerolysin, which was found to activate the inflammasome via pore formation on the plasma membrane (21). The illustration of the biochemical properties and functions of the pores (channels) formed in lysosomes by $\beta\gamma$ -CAT will be an interesting question to be solved.

Aerolysin-like PFTs are bacterial virulence factors that contribute to the spread of, and infection by, several important pathogens (12). Interestingly, various proteins containing aerolysin domains that undergo fusion with other domains have been discovered in vertebrates (9) (Table S1 and Fig. S14). Although a non-vertebrate-derived β -PFT-like protein has been shown to be involved in defense against parasite infection (33), the biological functions of vertebrate-derived aerolysin-containing proteins remain uncharacterized. $\beta\gamma$ -CAT represents a good example of an aerolysin-like fold that can be used either by bacteria for attack or by vertebrates for defense against infection, similar to the situation among vertebrate complement components C8, C9, and perforin and bacterial cholesterol-dependent cytolysin-like PFTs (34). The TFF domain is highly conserved in vertebrates, and TFFs harboring one to four TFF domains have been identified in species from frogs to humans (15–17). Several lines of evidence suggest possible roles for TFFs in the modulation of the host immune system (18, 19), but the actions by which TFFs exert their biological activities are still largely unknown. It would be very interesting to investigate whether TFFs function via combination with partners, such as aerolysin-like proteins, from either the host or microbes to modulate host antimicrobial and immune responses in other vertebrate species, including mammals.

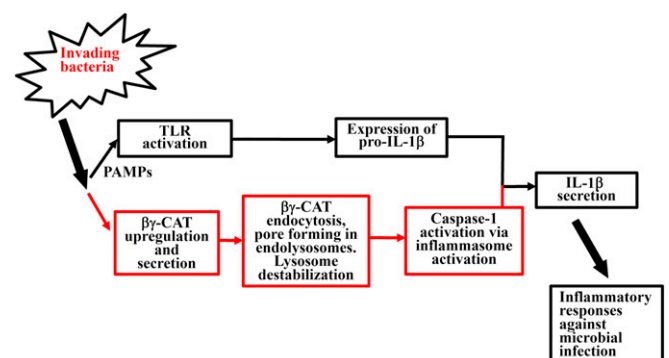


Fig. 5. The proposed action of $\beta\gamma$ -CAT during bacterial infection. Upon bacterial infection, pathogen-associated molecular patterns (PAMPs) induce the activation of TLRs (37), which may subsequently induce the intracellular production of pro-IL-1 β (4). Additionally, the action of $\beta\gamma$ -CAT, a host-derived bacterial PFT-like protein and TFF complex, was proposed as indicated.

In conclusion, the present work illustrated the ability of $\beta\gamma$ -CAT, an aerolysin-like protein and TFF complex, to protect the host from microbial infection (Fig. 5). This role could be at least partially explained by the IL-1 β release and innate immune cell recruitment triggered by $\beta\gamma$ -CAT. Pore formation by the protein in lysosomes may lead to IL-1 β maturation and release via inflammasome activation. This protein complex should thus play an important role in initiating and regulating immune responses to eliminate microbial invasion. Our findings could serve as clues in investigating the possible occurrence of similar antimicrobial strategies, the effective molecules, and the action mechanisms involved in vertebrates. Such studies will eventually help to illustrate human pathophysiological mechanisms and to develop novel therapeutics for related diseases.

Materials and Methods

Animals. Frogs (*B. maxima*) with a mean body weight of 25 ± 5 g were caught in their natural environment. The frogs were placed into tanks filled with dechlorinated tap water between 20 °C and 24 °C for 1 wk before the experiments. These tanks were equipped with four platforms, and four animals were placed into each tank. The frogs were fed live *Tenebrio molitor*. Kunming mice were also used in the experiments and are described in the *SI Materials and Methods*. All procedures and the care and handling of animals were approved by the Ethics Committee of the Kunming Institute of Zoology, the Chinese Academy of Sciences.

Purification of $\beta\gamma$ -CAT. The purification of $\beta\gamma$ -CAT was according to the method described previously (10), and the purity of the protein purified was

analyzed by native-PAGE and SDS/PAGE with silver staining (*SI Materials and Methods* and Fig. S5).

In Vivo and in Vitro Frog Experiments. Frogs were injected intraperitoneally with 1×10^9 cfu per frog (to determine the survival rate) or 1×10^8 cfu per frog (to count bacteria) *Comamonas* sp. in 0.1 mL of sterile 0.9% NaCl. The i.p. injection was performed as previously described (35). Each group contained 10 adult frogs. To assess the influence of $\beta\gamma$ -CAT on the frogs' survival rate or peritoneal bacterial counts, the frogs were intraperitoneally injected with $\beta\gamma$ -CAT (40 μ g/kg) in 0.1 mL of sterile 0.9% NaCl 4 h before infection. The sampling for Western blotting, bacterial counting, and flow cytometry is described in *SI Materials and Methods*. The in vitro experiments on frogs are described in *SI Materials and Methods* and Table S4.

In Vivo and in Vitro Experiments in Mice. The in vivo mouse experiments were performed as previously described (36) (*SI Materials and Methods*).

Statistical Analysis. Survival data were analyzed using the Kaplan–Meier method, and survival curves were compared using the log-rank test in univariate analysis. All other data are presented as the mean \pm SD. Two-sample comparisons were performed using Student *t* test. All other materials and methods are described in *SI Materials and Methods*.

ACKNOWLEDGMENTS. We thank Dr. Shaoxing Dai (Kunming Institute of Zoology) for his help with the bioinformatics analysis. This work was supported by Chinese 973 Program Grant 2010CB529800, Natural Science Foundation of China (NSFC–Yunnan joint Grant U1132601, NSFC Grants 31270835 and 31301884, and Chinese Academy of Sciences Grant KJZD-EW-L03.

- Beutler B (2004) Innate immunity: An overview. *Mol Immunol* 40(12):845–859.
- Medzhitov R (2010) Inflammation 2010: New adventures of an old flame. *Cell* 140(6):771–776.
- Dinarello CA (2009) Immunological and inflammatory functions of the interleukin-1 family. *Annu Rev Immunol* 27:519–550.
- Sims JE, Smith DE (2010) The IL-1 family: Regulators of immunity. *Nat Rev Immunol* 10(2):89–102.
- Chen GY, Nuñez G (2010) Sterile inflammation: Sensing and reacting to damage. *Nat Rev Immunol* 10(12):826–837.
- Strowig T, Henao-Mejia J, Elinav E, Flavell R (2012) Inflammasomes in health and disease. *Nature* 481(7381):278–286.
- Medzhitov R, Schneider DS, Soares MP (2012) Disease tolerance as a defense strategy. *Science* 335(6071):936–941.
- Zhao F, et al. (2014) Comprehensive transcriptome profiling and functional analysis of the frog (*Bombina maxima*) immune system. *DNA Res* 21(1):1–13.
- Szczesny P, et al. (2011) Extending the aerolysin family: From bacteria to vertebrates. *PLoS ONE* 6(6):e20349.
- Liu SB, et al. (2008) A novel non-lens betagamma-crystallin and trefoil factor complex from amphibian skin and its functional implications. *PLoS One* 3(3):e1770.
- Gao Q, et al. (2011) Characterization of the $\beta\gamma$ -crystallin domains of $\beta\gamma$ -CAT, a non-lens $\beta\gamma$ -crystallin and trefoil factor complex, from the skin of the toad *Bombina maxima*. *Biochimie* 93(10):1865–1872.
- Bischofberger M, Iacovache I, van der Goot FG (2012) Pathogenic pore-forming proteins: Function and host response. *Cell Host Microbe* 12(3):266–275.
- Los FC, Randis TM, Aroian RV, Ratner AJ (2013) Role of pore-forming toxins in bacterial infectious diseases. *Microbiol Mol Biol Rev* 77(2):173–207.
- Ogawa M, Takahashi TC, Takabatake T, Takeshima K (1998) Isolation and characterization of a gene expressed mainly in the gastric epithelium, a novel member of the ep37 family that belongs to the betagamma-crystallin superfamily. *Dev Growth Differ* 40(5):465–473.
- Taupin D, Podolsky DK (2003) Trefoil factors: Initiators of mucosal healing. *Nat Rev Mol Cell Biol* 4(9):721–732.
- Kjellef S (2009) The trefoil factor family: Small peptides with multiple functionalities. *Cell Mol Life Sci* 66(8):1350–1369.
- Zhang Y, et al. (2011) Activation of protease-activated receptor (PAR) 1 by frog trefoil factor (TFF) 2 and PAR4 by human TFF2. *Cell Mol Life Sci* 68(22):3771–3780.
- Wills-Karp M, et al. (2012) Trefoil factor 2 rapidly induces interleukin 33 to promote type 2 immunity during allergic asthma and hookworm infection. *J Exp Med* 209(3):607–622.
- Shah AA, et al. (2012) Increased susceptibility to *Yersinia enterocolitica* infection of Tff2 deficient mice. *Cell Physiol Biochem* 30(4):853–862.
- Qian JQ, Liu SB, He YY, Lee WH, Zhang Y (2008) Acute toxicity of betagamma-CAT, a naturally existing non-lens betagamma-crystallin and trefoil factor complex from frog *Bombina maxima* skin secretions. *Toxicol* 52(1):22–31.
- Gurcel L, Abrami L, Girardin S, Tschopp J, van der Goot FG (2006) Caspase-1 activation of lipid metabolic pathways in response to bacterial pore-forming toxins promotes cell survival. *Cell* 126(6):1135–1145.
- Mariathasan S, et al. (2006) Cryopyrin activates the inflammasome in response to toxins and ATP. *Nature* 440(7081):228–232.
- Misawa T, et al. (2013) Microtubule-driven spatial arrangement of mitochondria promotes activation of the NLRP3 inflammasome. *Nat Immunol* 14(5):454–460.
- Hornung V, et al. (2008) Silica crystals and aluminum salts activate the NALP3 inflammasome through phagosomal destabilization. *Nat Immunol* 9(8):847–856.
- Rollins-Smith LA, Ramsey JP, Pask JD, Reinert LK, Woodhams DC (2011) Amphibian immune defenses against chytridiomycosis: Impacts of changing environments. *Integr Comp Biol* 51(4):552–562.
- Lai R, et al. (2002) Antimicrobial peptides from skin secretions of Chinese red belly toad *Bombina maxima*. *Peptides* 23(3):427–435.
- Lee WH, et al. (2005) Variety of antimicrobial peptides in the *Bombina maxima* toad and evidence of their rapid diversification. *Eur J Immunol* 35(4):1220–1229.
- Schroder K, Tschopp J (2010) The inflammasomes. *Cell* 140(6):821–832.
- Robert J, Ohta Y (2009) Comparative and developmental study of the immune system in *Xenopus*. *Dev Dyn* 238(6):1249–1270.
- Jaenicke R, Slingsby C (2001) Lens crystallins and their microbial homologs: Structure, stability, and function. *Crit Rev Biochem Mol Biol* 36(5):435–499.
- Cole AR, et al. (2004) Clostridium perfringens epsilon-toxin shows structural similarity to the pore-forming toxin aerolysin. *Nat Struct Mol Biol* 11(8):797–798.
- Gao Q, et al. (2011) $\beta\gamma$ -CAT, a non-lens betagamma-crystallin and trefoil factor complex, induces calcium-dependent platelet apoptosis. *Thromb Haemost* 105(5):846–854.
- Galinier R, et al. (2013) Biomphalysin, a new β pore-forming toxin involved in *Biomphalaria glabrata* immune defense against *Schistosoma mansoni*. *PLoS Pathog* 9(3):e1003216.
- Rosado CJ, et al. (2007) A common fold mediates vertebrate defense and bacterial attack. *Science* 317(5844):1548–1551.
- Cosma CL, Swaim LE, Volkman H, Ramakrishnan L, Davis JM (2006) Zebrafish and frog models of *Mycobacterium marinum* infection. *Curr Protoc Microbiol* Chapter 10:Unit 10B 12.
- Xiang Y, et al. (2013) Adenosine-5'-triphosphate (ATP) protects mice against bacterial infection by activation of the NLRP3 inflammasome. *PLoS ONE* 8(5):e63759.
- Medzhitov R, Preston-Hurlburt P, Janeway CA, Jr. (1997) A human homologue of the *Drosophila* Toll protein signals activation of adaptive immunity. *Nature* 388(6640):394–397.